

# Helium-Three in Aerogel

W.P. Halperin and J.A. Sauls

*Department of Physics and Astronomy, Northwestern University, Evanston, Illinois 60208*

(Dated: Version October 22, 2018)

Liquid  $^3\text{He}$  confined in silica aerogel provides us with a unique system to study the effects of quenched disorder on the properties of a strongly correlated quantum liquid. The superfluid phases display interplay between disorder and complex symmetry-breaking.

## Introduction

The discovery of the superfluid phases of  $^3\text{He}$  led to experimental and theoretical developments that have found deep influence on many aspects of condensed matter physics. The original observations were acknowledged with Nobel prizes in 1996 to Douglas Osheroff, Robert Richardson and David Lee [1], and this past year for the theoretical work [2] of Anthony Leggett that developed hand-in-hand with the early experimental investigations of these phases. The transition from normal to superfluid is a second order thermodynamic transition that was detected because of a discontinuous jump in heat capacity. The line of phase transitions that marks the onset of superfluidity is shown as the continuous red curve extending from  $P = 0 - 35$  bar in Fig. 1. Contrast this curve with the blue data for 'dirty' superfluid  $^3\text{He}$ , showing that the effects of impurities are to suppress the transitions and to create a zero temperature critical pressure.

At relatively high temperatures, the normal state of liquid  $^3\text{He}$  is well described by Landau's Fermi liquid theory, formulated in terms low-lying excitations, called "quasi-particles", which are composite states of  $^3\text{He}$  atoms with spin  $\frac{1}{2}$  and fermion number 1 [3]. Strong interactions also lead to Bosonic excitations, e.g. phonons and spin-waves, but the fermionic excitations dominate many of the low-temperature thermodynamic and transport properties, including the specific heat, thermal conductivity, magnetization and diffusion coefficient. At very low temperatures liquid  $^3\text{He}$  exhibits a phase transition from a classic Fermi liquid state to a unique superfluid that is a paradigm for many newly discovered "unconventional" superconductors [4] in which one or more symmetries of the normal Fermi liquid state (e.g. rotations, time-inversion, etc.) are spontaneously broken in conjunction with the broken  $U(1)$  gauge symmetry that is characteristic of superconductivity. The ordered phases of pure superfluid  $^3\text{He}$  are summarized in a "sidebar".

We can often obtain important information about new states of matter by examining how their properties are modified by external influences. For example, the effects of impurities and surfaces have played an important role in revealing basic properties of the high temperature superconductors, such as the nature of the order parameter

[5, 6], and they provide the key elements in applied areas of superconductivity where flux pinning and critical currents are important.

Usually impurities and defects are unavoidable. However, in contrast to metals, liquid  $^3\text{He}$  naturally expels impurities, even isotopic impurities, which makes it the purest and most homogeneous condensed matter system, and one that, until recently, could not be perturbed in a way that is typical of superconductors where chemical impurities can be easily inserted into the structure. In fact, some superconducting materials, have chemical and physical imperfections which mask their intrinsic behavior.

In an earlier Physics Today article Chan et al. [7] describe the properties of superfluid  $^4\text{He}$  inside aerogel, notably the non-universal critical behavior of superfluid  $^4\text{He}$  and the change of the phase diagram for mixtures  $^4\text{He}$  and  $^3\text{He}$ . At that time the observation of superfluidity of  $^3\text{He}$  in aerogel had just been made; more extensive work has followed and is the subject of this article.

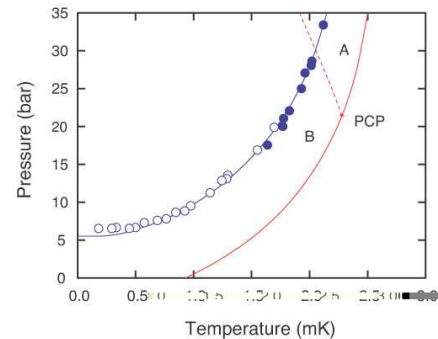


FIG. 1: Pressure vs. temperature phase diagram. The superfluid transition line for pure  $^3\text{He}$  is the smooth red curve extending from  $P = 0 - 35$  bar. The A-B transition for bulk  $^3\text{He}$  is shown as a dashed red line. Shown here are the transitions for superfluid  $^3\text{He}$  in 98% aerogel from Cornell [8] (open circles) and Northwestern [9] (solid circles). There are modest variations in this phase diagram from one aerogel sample to another at the same porosity. The solid blue curve is a theoretical calculation of the transition based on the scattering model [10, 11].

### Phases of Pure Superfluid $^3\text{He}$

The superfluid phases of  $^3\text{He}$  are Bardeen-Cooper-Schrieffer condensates of p-wave ( $L = 1$ ) Cooper pairs with orbital wave functions that are linear superpositions of the p-wave states:  $\Psi_{1,1}(\mathbf{r}) = (x + iy)/\sqrt{2}$ ,  $\Psi_{1,-1}(\mathbf{r}) = (x - iy)/\sqrt{2}$ ,  $\Psi_{1,0}(\mathbf{r}) = z$ . The Pauli exclusion principle then requires that these pairs form nuclear spin-triplet states ( $S = 1$ ). There are three superfluid phases of pure  $^3\text{He}$  corresponding to different realizations of the p-wave, spin-triplet manifold. Two phases, the A and B phases, are indicated in the phase diagram in Fig. 1. A third phase, called the  $A_1$  phase, develops in a narrow region near  $T_c$  in an applied magnetic field. All three phases are characterized by their nuclear spin structure and correspond to different superpositions of p-wave, spin-triplet states. The  $A_1$  phase is the spin-polarized state,  $|A_1\rangle = \Psi_{1,1}(\mathbf{r})|\uparrow\uparrow\rangle$ , and has the highest transition temperature in a magnetic field. The A phase is a superposition with equal amplitudes for the oppositely polarized spin-triplet states (referred to as “equal spin pairing”),  $|A\rangle = \Psi_{1,1}(\mathbf{r})(|\uparrow\uparrow\rangle + |\downarrow\downarrow\rangle)/\sqrt{2}$ . The A phase survives in large magnetic fields without destroying Cooper pairs by conversion of  $|\downarrow\downarrow\rangle$  pairs into  $|\uparrow\uparrow\rangle$  pairs in order to accommodate the nuclear Zeeman energy. The B phase, which is the stable state over most of the phase diagram in zero magnetic field, is a superposition of all three triplet spin states:  $|B\rangle = \Psi_{1,-1}(\mathbf{r})|\uparrow\uparrow\rangle + \Psi_{1,1}(\mathbf{r})|\downarrow\downarrow\rangle + \Psi_{1,0}(\mathbf{r})|\uparrow\downarrow + \downarrow\uparrow\rangle$ . One of the key signatures of a B-like phase is the reduction of the nuclear magnetic susceptibility resulting from the  $|\uparrow\downarrow + \downarrow\uparrow\rangle$  pairs. The B phase is suppressed in large magnetic fields when the Zeeman energy is comparable to the binding energy of the  $|\uparrow\downarrow + \downarrow\uparrow\rangle$  pairs. The transition from A to B phases is first order and is accompanied by a latent heat. This transition exhibits supercooling, but no superheating. The point in the phase diagram where all three phases are degenerate is called the polycritical point (PCP). This singular point is destroyed by application of a magnetic field which opens up regions of stability of both the A and  $A_1$  phases over the full pressure range. Many of these features are fundamentally altered in the presence of disorder.

### Aerogel

In the past decade it was found [12, 13] that impurities can be introduced into  $^3\text{He}$  by impregnating the liquid into the open structure of silica aerogel. These are extremely porous, low-density materials (as can be seen in Fig. 2), with porosities up to 99.5% by volume, formed as a dilute network of thin silica strands having a typical thicknesses of 3-5 nm [14]. Aerogels are fascinating materials that have found practical applications, e.g. as Cerenkov counters in particle physics and as light weight transparent thermal insulation. Figure 2 is a photograph of three silica aerogels with widely ranging porosities. The aerogels are transparent, clearly evident for the most porous sample on the right. One can infer that the structure is homogeneous on length scales of order the wavelength of visible light.

Silica aerogel is formed from a synthesis of silica clusters approximately  $\delta = 3$  nm in diameter. Gelation is performed from tetramethylorthosilicate and the clusters aggregate to generate the strands that form the final gel structure. The wet gel is dried at a supercritical pressure in a high pressure autoclave to avoid collapse of the microstructure from capillary forces at the liquid-gas interface. The resulting material is air stable and hydrophobic. Small angle X-ray measurements [7, 15] indicate that there are fractal correlations characteristic of the process of diffusion-limited cluster aggregation over a decade or more in wavevector. Density correlations are observed to onset at  $q_a^{-1} \simeq 10 - 30$  nm in the structure factor. The aerogel correlation length,  $\xi_a = \pi/q_a$ , is identified as the typical distance between silica strands or clusters,  $\xi_a \approx 30 - 100$  nm. At longer length scales the aerogel



FIG. 2: Photograph of three silica aerogel samples with porosities 95%, 98%, and 99% from left to right, placed on the top of a five inch diameter high pressure autoclave used to supercritically dry the samples. The light blue color is caused by Rayleigh scattering.

particle-particle correlations are random. These conclusions are supported by numerical simulations of a 98% porosity gel structure shown in Fig. 3 [16]. In the simulation an ensemble of particles, which is initially randomly distributed, executes Brownian motion until the particles aggregate by contact with one another. For the simulated structure shown in Fig. 3 a geometric mean free path of 200 nm was obtained as the average length of a straight line trajectory terminating on aerogel particles. This geometric mean free path is what one expects for the transport mean free path resulting from elastic scattering of  $^3\text{He}$  quasiparticles moving at constant speed through the pore space. The geometric mean free path is indeed comparable to the transport mean free paths,  $\lambda \approx 130 - 180$  nm, that have been obtained from anal-

yses of transport measurements on liquid  $^3\text{He}$  (spin diffusion, acoustic attenuation, and thermal conductivity) performed in a 98% aerogel. The close comparison of these length scales provides support for the application of scattering theory to describe the effects of aerogel on the superfluid phases of  $^3\text{He}$ .

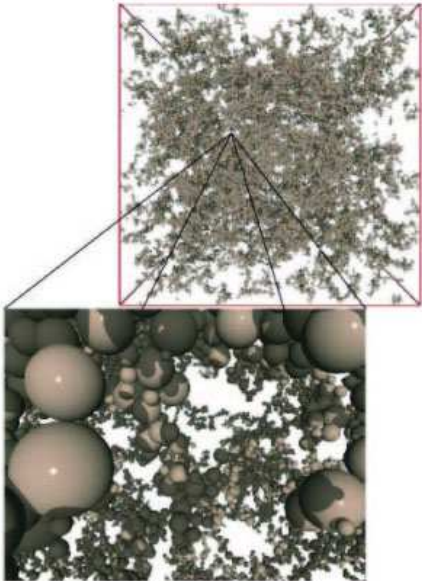


FIG. 3: Perspective view of a 98% porosity gel structure grown by numerical simulation [16] for a  $600 \times 600 \times 600 \text{ nm}^3$  volume beginning with a random suspension of particles having a log-normal distribution and mean diameter of 3 nm. The particles assemble in strands that are spatially correlated over distances of order 30 nm. The calculated geometric mean free path in this gel was found to be 200 nm.

### $^3\text{He}$ with Quenched Disorder

When impregnated with  $^3\text{He}$ , the aerogel is found to have a dramatic effect on the properties of liquid  $^3\text{He}$ . The superfluid transition temperature,  $T_c$ , is suppressed well below the bulk value for all pressures [12, 13], and there is a zero-temperature, “quantum” phase transition [8] at  $p_c \simeq 6$  bar, for a 98% porous aerogel, separating a disordered normal Fermi-liquid phase from a superfluid phase with very different properties than that of pure  $^3\text{He}$ . Quenched disorder leads to new physical behavior in a quantum liquid with complex symmetry breaking. Its detailed study may help us better understand the pure phases of  $^3\text{He}$  as well as strongly correlated electronic materials with unconventional pairing.

The two length scales,  $\delta$  and  $\xi_a$ , characteristic of the structure of aerogel are identified in the sketch shown in Fig. 4. These length scales are much larger than the Fermi wavelength of  $^3\text{He}$  quasiparticles,  $\approx 0.1$  nm. Consequently, to an excellent approximation, the basic prop-

erties of the normal Fermi liquid in the open volume, such as the density, effective mass and quasiparticle interactions, are essentially unaffected by the aerogel. This is not the case for the superfluid phase. Here the important length is the coherence length of pure superfluid  $^3\text{He}$  (the size of a Cooper pair),  $\xi \approx 80$  nm at low pressure, which is comparable to the aerogel correlation length,  $\xi_a$ . One expects significant effects on the phase diagram and structure of the Cooper pair condensates in such a confined geometry.

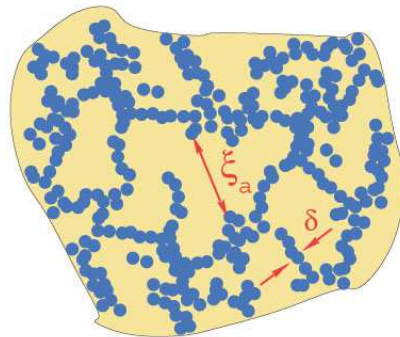


FIG. 4: A sketch of silica aerogel showing low-density regions containing  $^3\text{He}$  (yellow) threaded by higher density strands and aggregates of silica (blue). Two principal length scales are indicated: the typical size of the aerogel strands,  $\delta \simeq 3$  nm, and the aerogel correlation length,  $\xi_a \simeq 30$  nm, identified as the average inter-strand distance.

In pure, bulk  $^3\text{He}$  inelastic binary collisions between quasiparticles limits the transport of heat, momentum and magnetization. Elastic scattering is absent, except at ultra-low temperatures when boundary scattering from the containing walls limits ballistic propagation of quasiparticles. Aerogel changes this situation. At temperatures below  $T^* \approx 10$  mK *elastic* scattering of quasiparticles by the aerogel dominates *inelastic* quasiparticle-quasiparticle collisions [17]. Elastic scattering limits the mean free path of normal  $^3\text{He}$  quasiparticles to  $\lambda \simeq 130 - 180$  nm for aerogels with 98% porosity. Thus, the low-temperature limits for the transport coefficients are determined by scattering from the aerogel. Consequently, transport processes in  $^3\text{He}$  are similar to those typical of metals at low temperatures. Experimental measurements for  $T \ll T^*$  provide a direct determination of the transport mean free path. Once it is determined we can make quantitative predictions for the thermodynamic and transport properties of the superfluid phase of  $^3\text{He}$  in aerogel, and test the scattering theory.

### Normal-state transport

In the normal state of pure liquid  $^3\text{He}$ , the quasiparticle lifetime, or mean free path, is determined by the inelastic collision rate between quasiparticles [18],

$$\frac{1}{\tau_{\text{in}}} = \langle W \rangle \frac{(k_B T)^2}{E_f} \propto T^2, \quad (1)$$

where  $\langle W \rangle$  is the transition probability for quasiparticle scattering on the Fermi surface and  $E_f$  is the Fermi energy [3]. For  $^3\text{He}$  in aerogel, binary collisions dominate at relatively high temperatures, while elastic scattering of quasiparticles from the aerogel strands leads to a temperature-independent scattering rate at low temperatures ( $T < T^*$ ). The latter is determined by the transport mean free path,  $\lambda$ , where

$$\frac{1}{\tau_{\text{el}}} = (v_f/\lambda), \quad (2)$$

and  $v_f$  is the Fermi velocity. A good illustration of the cross-over is provided by the transport of magnetization in the hydrodynamic limit, given by the spin current density,

$$\mathbf{j}_M = -D_M \nabla M, \quad (3)$$

where  $M$  is the local magnetization and  $D_M$  is the spin diffusion coefficient.

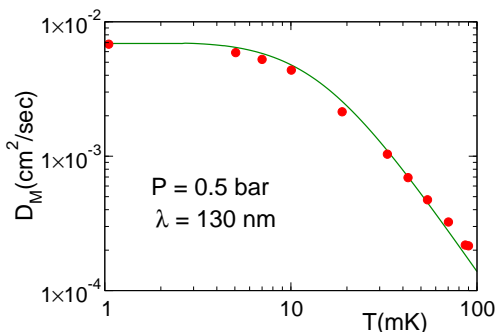


FIG. 5: Comparison of the theory to experimental data taken at Grenoble [19]. The inelastic scattering rate is fit to the high-temperature data. The elastic transport mean free path obtained from the fit is  $\lambda = 130$  nm.

The diffusion coefficient can be calculated from Landau's kinetic theory of quasiparticles, with the collision integral determined by both elastic scattering from the aerogel medium and inelastic collisions between quasiparticles. The general solution has the form,

$$D_M = \frac{1}{3} v_f^2 (1 + F_0^a) \tau_D, \quad (4)$$

in the hydrodynamic limit,  $\omega_L \ll \tau_D^{-1}$ , where  $\omega_L = \gamma B$  is the Larmor frequency,  $\tau_D^{-1}$  is the collision rate that limits the transport of magnetization and  $F_0^a$  is the exchange

interaction for liquid  $^3\text{He}$ . The diffusion coefficient has been calculated from an exact solution of the Landau-Boltzmann transport equation including both scattering channels [20].

Measurements of the spin-diffusion coefficient for  $^3\text{He}$  in 98% aerogel performed in Grenoble [19] are shown in Fig. 5 for  $P = 0.5$  bar. The spin-diffusion coefficient decreases as  $D_M \propto T^{-2}$  at high temperatures and coincides with measurements of the spin-diffusion coefficient for bulk  $^3\text{He}$  [21]. At low temperature there is a cross-over to the elastic scattering regime determined by the aerogel. The mean-free path is found to be  $\lambda = 130$  nm for this 98% aerogel.

### Aerogel Scattering

The fact that the superfluid coherence length is much larger than the silica strand dimensions and comparable to or larger than the aerogel correlation length, at least at lower pressures, suggested that a theory based on atomic scale scattering centers might provide an adequate description of the effects of the aerogel on the properties of superfluid  $^3\text{He}$ . A theoretical approach based on scattering by point impurities, analogous to the Abrikosov-Gorkov theory of disorder in superconductors [22], was developed by Thuneberg *et al.* [10] in an effort to account for the observed behavior. Elastic scattering by impurities and defects results in diffusive transport in the normal Fermi liquid state, and to substantial corrections to the transition temperature, order parameter, quasiparticle excitation spectrum, superfluid density, magnetization, etc. In its simplest form the theory assumes that elastic scattering of  $^3\text{He}$  quasiparticles by the silica aerogel is isotropic and homogeneous; this is referred to as the homogeneous, isotropic, scattering model (HISM). Extensions of the theory [10, 11] to include inhomogeneities of the scattering medium, referred to as inhomogeneous, isotropic scattering models (IISM), are required when aerogel structural correlations are comparable to or larger than the coherence length, as is the situation at higher pressures.

Elastic scattering of quasiparticles is deleterious to an unconventional superfluid, like  $^3\text{He}$ . The fragility of non- $s$ -wave pairing holds for superfluid  $^3\text{He}$  as well as for a number of superconducting compounds, including the heavy fermion superconductor  $\text{UPt}_3$  ( $f$ -wave), the copper oxide superconductors ( $d$ -wave),  $\text{Sr}_2\text{RuO}_4$  ( $p$ -wave) and possibly several organic superconductors. Scattering from impurities reduces the coherence between pairs of quasiparticles that bind to form Cooper pairs, thus reducing the transition temperature and suppressing the magnitude of the order parameter. The Abrikosov-Gorkov theory, originally developed for magnetic scattering in conventional isotropic superconductors, is easily generalized to describe Cooper pair breaking in unconventional

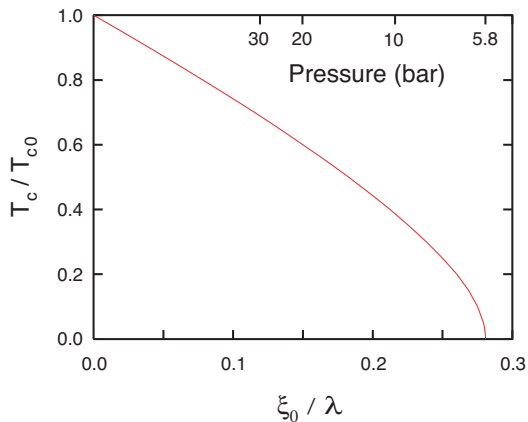


FIG. 6: The reduction of the transition temperature of an unconventional superconductor with coherence length,  $\xi_0$ , owing to elastic scattering of Fermi quasi-particles with mean free path  $\lambda$ . The pressure scale was calculated for  $\lambda = 140$  nm.

(non-*s*-wave) superfluids for magnetic or non-magnetic impurity scattering.

In the HISM the pair breaking parameter that determines the suppression of the transition temperature is the ratio of the pure superfluid coherence length to the transport mean free path,  $\xi_0/\lambda$ . In fact the critical pressure ( $p_c \simeq 6$  bar) shown in Fig. 1 for a 98% porous aerogel corresponds to the critical pair-breaking parameter shown in Fig. 6, i.e.  $\xi_0(p_c)/\lambda = 0.28$ . For  $^3\text{He}$  in aerogel the limiting mean free path is a constant, independent of pressure, fixed by the aerogel structure. But the coherence length at zero temperature,  $\xi_0 = \hbar v_f / 2\pi k_B T_{c0}$ , varies from 77 nm at low pressure to 16 nm at the highest pressures near the melting curve. For a mean free path of 140 nm, which is close to the value obtained from the spin-diffusion measurements for the 98% aerogel used by the Grenoble group, we can account for the observed critical pressure, and implicitly from the theory we obtain the pressure scale shown on the upper axis of Fig. 6. Rotating Fig. 6 clockwise by 90 degrees shows the qualitative agreement with the experimental phase diagram for  $^3\text{He}$  in aerogel shown in Fig. 1. The HISM provides a reasonable description of the dirty superfluid at low pressures; it accounts semi-quantitatively for the reduction of  $T_c$ , including the critical pressure,  $p_c$ , and the pair-breaking suppression of the order parameter [10, 17]. However, the HISM underestimates the transition temperature at higher pressures and higher porosities where the pair size is comparable to, or smaller than, the typical distance between aerogel strands. This failure of the HISM is most evident in the pressure dependence of  $T_c$  [10, 23].

The qualitative picture of the correlated aerogel is a random distribution of low density regions, ‘voids’, with a typical dimension of  $\xi_a$ . These low-density regions are available for formation of the condensate at higher

temperatures. In the limit  $\xi_0 \ll \xi_a$ , the suppression of the superfluid transition is determined by a new pair-breaking parameter, proportional to  $(\xi_0/\xi_a)^2$ . In the opposite limit, when the pair size is much larger than  $\xi_a$ , the aerogel is effectively homogeneous on the scale of the pairs and pair-breaking results from homogeneous scattering defined by the pair-breaking parameter  $(\xi_0/\lambda)$ . This latter limit is achieved at low pressures. Theoretical analyses which include the effects of aerogel correlations [10, 11, 24] provide a quantitative description of the phase diagram, as well as the order parameter, excitation spectrum and transport properties of  $^3\text{He}$  in aerogel over the whole pressure range.

## Superfluidity

A powerful technique that is sensitive to the onset of superfluidity makes use of a high-Q torsional oscillator. The torsion rod is attached perpendicular to a disk containing the helium sample. Using this approach, Porto and Parpia at Cornell [12] found that the period of the oscillator shifted with an abrupt onset at specific temperatures depending on the pressure. The method relies on the fact that the normal fluid is viscously clamped to the porous structure; but since the superfluid has zero viscosity it does not contribute to the moment of inertia. At the onset of superfluidity there is a sharp decrease of oscillation period. The loss of inertia is quantitatively interpreted in terms of the superfluid density, shown in Fig. 7. In contrast with pure superfluid  $^3\text{He}$  the superfluid

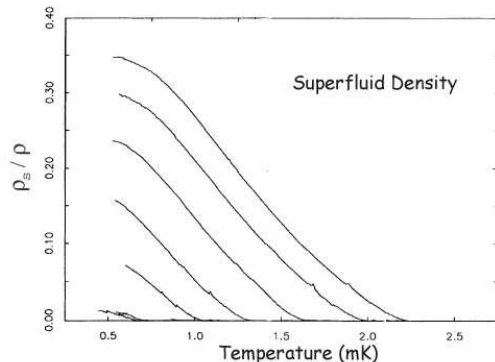


FIG. 7: The superfluid fraction as determined from torsional oscillator measurements from the Cornell group [12]. Measurements at pressures of (from lowest to highest) 3.4, 5.0, 7.0, 10, 15, 25 bar. The superfluid fraction is smaller than that of pure  $^3\text{He}$  which approaches  $\rho_s/\rho = 1$  as  $T \rightarrow 0$ .

fraction is much less than unity, a direct reflection of the pair-breaking effect of scattering off the aerogel. Shortly after these measurements were performed the group at Northwestern [13] observed the sharp onset of frequency shifts in the nuclear magnetic resonance (NMR) spec-

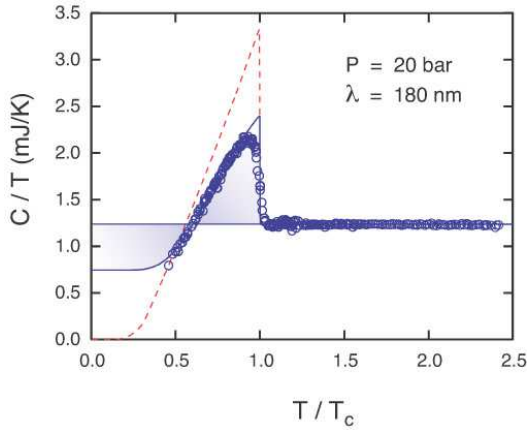


FIG. 8: The heat capacity of  $^3\text{He}$  in a 98% porous silica aerogel. The measurements, performed at Northwestern University, show the transition to the superfluid state as a jump in the heat capacity which is reduced by a factor of 0.55 compared to that of pure superfluid  $^3\text{He}$  at the same pressure of 20 bar (dashed red curve).

trum, qualitatively similar to those associated with the superfluid phase in pure  $^3\text{He}$ . But in the case of  $^3\text{He}$  in aerogel the shifts were significantly reduced in magnitude. The reduction of NMR frequency shifts and superfluid fraction compared to pure  $^3\text{He}$  provides a consistent picture for the reduction of the magnitude of the order parameter. This fact is directly confirmed in measurements of the heat capacity.

Heat capacity experiments [25], shown in Fig. 8 for a pressure of 20 bar, demonstrate that the superfluid transition has a discontinuity similar to that of a BCS superconductor. For pure superfluid  $^3\text{He}$  the size of the discontinuity is larger than the predicted BCS result of  $\Delta C/C = 1.43$ . Strong coupling effects are responsible for specific heat jumps as large as  $\Delta C/C \simeq 2.0$  near melting pressure. Direct comparison between pure superfluid  $^3\text{He}$  (dashed red curve) [26] and that of superfluid  $^3\text{He}$  in aerogel (shown in blue) indicates that the heat capacity discontinuity is substantially reduced, by a factor of 0.55 at a pressure of 20 bar, due to scattering by the aerogel. The reduction is even below that expected for the weak-coupling limit of a clean BCS superconductor. This is a consequence of two factors: (i) the decrease in the transition temperature leads to a reduction of strong coupling effects, proportional to  $T_c$ , and (ii) the pair-breaking effect increases the free energy and reduces the magnitude of the order parameter even in the weak coupling approximation [10].

### Thermal Conductivity

Heat transport by diffusion in pure superfluid  $^3\text{He}$  is masked by the propagation of heat via hydrodynamic

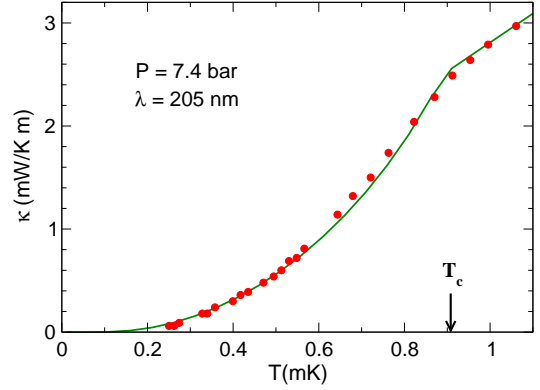


FIG. 9: Thermal conductivity data from the Lancaster group [28] (circles) at  $P = 7.4$  bar is compared with theory (solid curve). The theoretical calculation assumes a B-phase order parameter. A mean free path of  $\lambda = 205$  nm is obtained from the slope of the normal-state thermal conductivity. The theoretical results, including the value of  $T_c$  for this aerogel, are based on the same mean free path.

mode in which normal and superfluid components move counter to one another [27]. The presence of aerogel strongly reduces the mean free path for quasiparticle diffusion, and effectively clamps the hydrodynamic motion of the normal component in “dirty” superfluid  $^3\text{He}$ . Hydrodynamic heat flow is suppressed and heat transport is determined by quasiparticle diffusion.

Measurements of the thermal conductivity of  $^3\text{He}$  in 98% aerogel carried out at the University of Lancaster are shown in Fig. 9. The signature of the onset of superfluidity in thermal conductivity is the change in slope at  $T_c$ .

Scattering by the aerogel matrix leads to pair-breaking and the formation of a spectrum of low-energy quasiparticle states below the gap. In general the excitation spectrum depends upon the symmetry of the order parameter, as well as the scattering cross-section and mean-free path. The suppression of the thermal conductivity shown in Fig. 9 below that of the normal state is characteristic of elastic scattering and the suppression of the density of states for low-energy excitations. The measurements of the thermal conductivity of  $^3\text{He}$  in 98% aerogel at low pressures [28] are in good agreement with theoretical calculations based on either the B- or A-phase order parameters. At higher pressures, where pair-breaking effects are weaker, significant differences in the thermal conductivity for these two phases are predicted [29].

### Gapless Superfluid

In the strong scattering limit of the HISM a band of gapless excitations forms, *centered at the Fermi level*, with energies  $\varepsilon \leq \gamma \approx 0.67\Delta\sqrt{\xi_0/\lambda}$ . This band is rela-

tively insensitive to the symmetry of the order parameter, but depends on its magnitude,  $\Delta$ . The constant density of states for low-energy excitations,  $\varepsilon \ll \gamma$ , gives rise to a linear  $T$ -dependence of both the thermal conductivity and specific heat deep in the superfluid phase at very low temperatures,  $k_B T \ll \gamma$ .

Heat transport measurements by the low-temperature group at the University of Lancaster[30] have shown that the low-temperature limit of the thermal conductivity of superfluid  $^3\text{He}$  is linear in temperature, consistent with there being a significant density of gapless Fermion excitations near the Fermi level.

The third law of thermodynamics requires that the entropy of both the normal and superfluid states vanish at zero temperature. For a second-order transition the equality of the entropy for both normal and superfluid phases at  $T_c$  requires that the shaded areas in Fig. 8 to be equal. If we rule out an unphysical, non-monotonic, temperature dependence of the heat capacity at low temperatures, the equal-area constraint requires that there be a non-zero intercept for  $C/T$  at  $T = 0$ , as shown in Fig. 8. Consequently, the heat capacity must be linear in  $T$  at low temperatures. The intercept is directly proportional to the density of impurity-induced quasiparticle states at the Fermi level. For comparison, the B phase of pure superfluid  $^3\text{He}$  is fully gapped over the entire Fermi surface. The evidence is compelling from both of these thermal experiments that liquid  $^3\text{He}$  in aerogel is a gapless superfluid.

### Metastability

While it is widely accepted that a superfluid phase can exist in a sufficiently dilute aerogel, the precise nature of the superfluid phase is not fully resolved. Fundamental questions have been raised about the nucleation, stability and symmetry of phases that may be stabilized within the aerogel structure [9, 31, 32]. Theoretical calculations show that homogeneous and isotropic impurity scattering stabilizes the isotropic state (B phase) relative to the axial state (A phase) [10, 33]. This has been confirmed for 98% aerogels [34].

Nevertheless, early measurements of susceptibility and NMR frequency shifts indicated that an ESP state was observed, like the A phase in pure  $^3\text{He}$ . NMR experiments performed by the Stanford group have amplified on these earlier findings. They discovered [32] that on cooling there is a transition between two superfluid phases which is highly hysteretic and that the lower temperature phase has a decreased susceptibility, like the B phase (shown in Fig. 11), and that the higher temperature superfluid phase has a constant susceptibility like the A phase. This metastable A-phase region is shown shaded blue in Fig. 10. These conclusions were based on both observations of nuclear magnetic susceptibility obtained

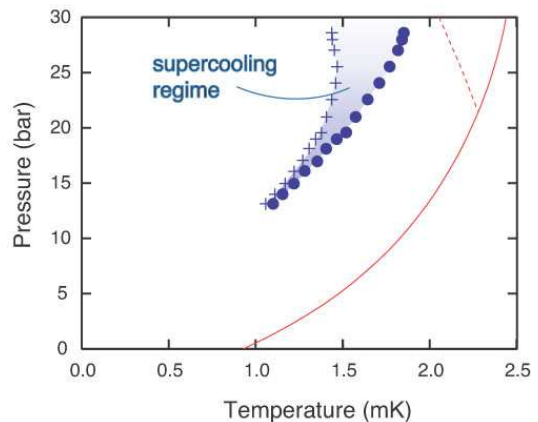


FIG. 10: The supercooled region of superfluid  $^3\text{He-A}$  in a 98% porous silica aerogel is shown in blue. The measurements are from Cornell [35].

from the integral of the NMR spectrum, as well as from abrupt NMR spectral shifts, which can be negative only in the case of an A phase. To account for hysteresis either the A phase supercools or the B phase superheats. Substantial effort has been directed to resolving which effect is dominant and what is the correct identification of these two phases. This includes work from laboratories at Stanford, Cornell, Northwestern, Lancaster, Osaka City University, University of Florida and the Kapitza Institute in Moscow.

The region of the phase diagram in question is shown in Fig. 10, taken from the Cornell measurements. Using transverse ultrasound the Northwestern group [9] showed that there is at most a tiny equilibrium sliver ( $\Delta T \simeq 20\mu\text{K}$ ) of A phase just below  $T_c$ , and that there is no PCP for  $^3\text{He}$  in 98% aerogel. They concluded that a B-like phase is stable over essentially all of the equilibrium phase diagram in zero field. How is it possible to have a supercooled A phase in zero magnetic field as shown in Fig. 10, if it is not thermodynamically stable at higher temperature? And if it is stable, why is this phase restricted to such a narrow interval below  $T_c$ ? This problem is not yet resolved and likely involves physical ideas for which there are no obvious parallels in pure superfluid  $^3\text{He}$ . Recently, the Stanford and Cornell experimenters found that the shaded region in Fig. 10 can, under certain conditions, sustain quasi-stable mixtures of A and B phases. Possibly the interfaces between the A and B-phase domains are pinned by the aerogel structure, reminiscent of impurity pinning of domain walls between magnetic phases or flux phases in other condensed matter systems.

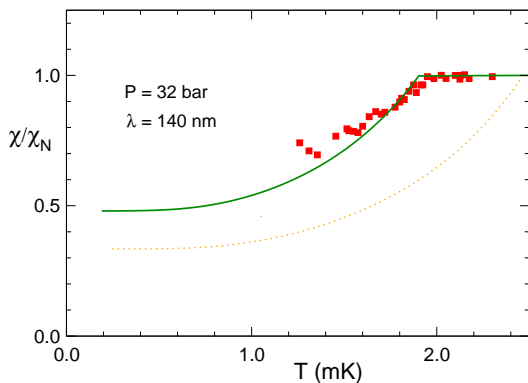


FIG. 11: Experimental data for the magnetic susceptibility of  ${}^3\text{He}$  in 98% aerogel at  $P = 32.0$  bar [32]. The solid green curve is the theoretical result for a “dirty B phase” with a mean-free path of  $\lambda = 140$  nm and a correlation length  $\xi_a = 40$  nm. The susceptibility of pure  ${}^3\text{He}$ -B is also shown for comparison (orange dotted curve).

### Magnetic Susceptibility

The nuclear magnetization of  ${}^3\text{He}$  played a central role in the identification of the spin-structure of the phases of pure superfluid  ${}^3\text{He}$ . For equal-spin-pairing (ESP) states, like the A phase, the magnetization is unchanged relative to that of the normal state since relative populations of the  $|\downarrow\downarrow\rangle$  and  $|\uparrow\uparrow\rangle$  pairs can be shifted without pair-breaking to accommodate the nuclear Zeeman energy. However for non-ESP phases like the B phase, the nuclear spin susceptibility is reduced by the formation of  $|\uparrow\downarrow + \downarrow\uparrow\rangle$  pairs.

Changes in the nuclear magnetization of superfluid  ${}^3\text{He}$  in aerogel are determined by competing effects of pairing correlations of quasiparticles with  $S_z = 0$ , and pair-breaking induced by scattering from the aerogel structure. In addition to the suppression of  $T_c$  by scattering from the aerogel, the magnitude of the susceptibility, particularly at low temperatures, is sensitive to the polarizability of the sub-gap excitations. Measurements of a B-like susceptibility in  ${}^3\text{He}$ -aerogel have been reported [13, 32]. Theoretical results for the susceptibility of superfluid  ${}^3\text{He}$  in aerogel with a B-phase order parameter were obtained [29, 36] and compared with the experimental results. Figure 11 shows measurements of the susceptibility from the Stanford group [32], as well as theoretical results for the susceptibility of a B-phase order parameter with aerogel correlation effects included within the effective pair-breaking model [11]. The aerogel strand correlations lead to both an increase in  $T_c$  and a decrease in the susceptibility due to a reduction in the sub-gap polarizability at low temperatures for the same mean free path.

### New Directions

#### *Fundamentally new phases in ${}^3\text{He}$ -aerogel?*

While there is support for the identification of the principal equilibrium superfluid phase in 98% aerogel as the dirty B phase, it is less certain that the orbital symmetry of the metastable phase is an A-like phase. There is less known about the energetics that governs the strong metastability of this phase. Theoretical understanding of defect structures in pure  ${}^3\text{He}$  give no *a priori* reason to assume that the stable or metastable phases of superfluid  ${}^3\text{He}$  should be simply related to the stable bulk phases of pure  ${}^3\text{He}$ . To the contrary, surface scattering and strong spatial variations of the order parameter imposed by scattering from an inhomogeneous distribution of aerogel strands and particles suggest that new phases, not realized in the bulk of pure  ${}^3\text{He}$ , may be stabilized in aerogel. This is certainly the case if the aerogel has significant orientational correlations on the coherence length scale. Long range orientational correlations of the silica strands scatter quasiparticles anisotropically and lead to anisotropic pair breaking. This implies the possibility of new phases reflecting the locally broken rotational symmetry of the aerogel. A theoretical suggestion for a new class of “robust” phases of  ${}^3\text{He}$  in aerogel that are stabilized by accommodating anisotropy in the scattering medium has been proposed [37]. Whether or not this phase or more complex structures are identified with the superfluid phase(s) of  ${}^3\text{He}$  in extremely porous aerogels ( $> 99\%$ ) requires new theoretical and experimental developments. Perhaps one of the more direct tests of these ideas is to impose anisotropy on a macroscopic scale within the aerogel. This would open up a new direction for the study of the orbital order parameter of  ${}^3\text{He}$ , analogous to the Zeeman coupling to the spin degrees of freedom of the order parameter. Indeed, such anisotropy can stabilize a two-dimensional planar or axial phase or a one-dimensional polar phase, depending on the nature of the induced anisotropy. Systematic studies of anisotropy-induced stabilization of new phases may also provide clues to the nature of the metastable phase in isotropic aerogels. For example, it is also possible that short-range anisotropic strand-strand correlations provide a mechanism for the stabilization or metastability of an A-like phase, even at pressures below the PCP of pure  ${}^3\text{He}$ .

#### *Does ${}^3\text{He}$ coating the aerogel strands lead to new physics?*

One of the early observations from NMR was the presence of a strong Curie susceptibility at milli-Kelvin temperatures. The origin of this magnetization is the localized  ${}^3\text{He}$  that forms one or two mono-layers of solid  ${}^3\text{He}$  on the surface of the silica strands. This solid  ${}^3\text{He}$



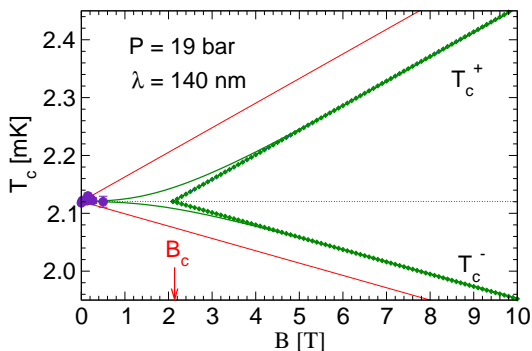


FIG. 12: Theoretical prediction for the nonlinear field evolution of the splitting of  $T_c$  with magnetic field for  ${}^3\text{He}$  in aerogel with a mean free path of  $\lambda = 140$  nm, a correlation length of  $\xi_a = 50$  nm and an anti-ferromagnetic exchange coupling of  $J \simeq 0.1$  mK (green lines). The splitting for  ${}^3\text{He}$ -aerogel without liquid-solid exchange is indicated by the solid (red) lines. The extrapolation of the high-field splitting to  $T_c(0)$  provides a direct measure of the exchange field,  $B_c \approx 2$  T (dark green lines). For a ferromagnetic coupling the exchange field would have the opposite sign.

can be removed by preferentially coating the silica with a few monolayers of  ${}^4\text{He}$ . But, the question arises as to whether or not the solid  ${}^3\text{He}$  spins play any significant role in scattering  ${}^3\text{He}$  quasiparticles and the process of pairing breaking. It is generally assumed, although direct evidence is sketchy, that for liquid  ${}^3\text{He}$  in contact with solid  ${}^3\text{He}$  there is an indirect exchange coupling between the  ${}^3\text{He}$  spins in the solid and the itinerant  ${}^3\text{He}$  quasiparticles of the liquid phase. Is this coupling present, and if so what is the sign and magnitude of the indirect exchange coupling?

Independent of the precise nature of the orbital state of superfluid  ${}^3\text{He}$  near  $T_c$ , the Zeeman coupling of a magnetic field to the spin-triplet Cooper pairs predicts a splitting of the phase transition in a magnetic field and stabilization of pure  $|\uparrow\uparrow\rangle$  Cooper pairs in a narrow temperature interval that increases linearly with the field,  $\Delta T_c \approx (60\mu\text{K}/\text{T})B$ . Indications of a solid-liquid exchange interaction come from low-field measurements of the phase diagram. For  ${}^3\text{He}$  in 98% aerogel it was found that there is no change in  $T_c$  and no evidence of a splitting of the transition for fields up to 0.8 Tesla [34]. Recent experiments at the University of Florida, in fields ranging from 5 to 15 Tesla, clearly show this splitting, but one which is smaller in the dirty superfluid compared to that in pure  ${}^3\text{He}$ .

If the splitting of the transition is suppressed in aerogel then a new mechanism must be at work that competes with the interaction responsible for the splitting of the transition in pure superfluid  ${}^3\text{He}$ . One possibility is the indirect exchange coupling with the solid  ${}^3\text{He}$  spins [11, 38]. This coupling gives rise to an additional term for the splitting, linear in the field, which can support or

compete with the intrinsic mechanism responsible for the splitting in pure  ${}^3\text{He}$ . Indeed for an anti-ferromagnetic exchange coupling of  $J \approx 0.1$  mK per  ${}^3\text{He}$  spin the low-field splitting,  $B < 1$  T, is suppressed. However, at higher fields the magnetization of the solid  ${}^3\text{He}$  will saturate and the splitting will appear for fields above the exchange field. Figure 12 shows the predicted evolution of the splitting at higher fields. Note that by extrapolating the linear splitting at high fields to  $T_c(B = 0)$  determines the exchange field,  $B_c$ , thus, providing a test of the theoretical proposal that indirect exchange between liquid and solid  ${}^3\text{He}$  in aerogel is present and modifies the phases of superfluid  ${}^3\text{He}$ . The presence of an indirect liquid-solid exchange coupling of this magnitude would open new directions for studying solid  ${}^3\text{He}$  magnetism in reduced dimensions, as well as a range of new low-field transport phenomena, in both the normal and superfluid phases, associated with spin-dependent scattering from polarized solid  ${}^3\text{He}$ .

#### *New phenomena of ${}^3\text{He}$ in aerogel?*

The impregnation of  ${}^3\text{He}$  in a solid structure which also suppresses the bulk transition provides possibilities for the study of proximity effects, mesoscopic transport and Josephson effects based on interfaces and weak links established between pure  ${}^3\text{He}$  and  ${}^3\text{He}$  confined in aerogel. Initial studies of nucleation and possible proximity effects between bulk superfluid  ${}^3\text{He}$  and  ${}^3\text{He}$ -aerogel have already opened up new questions about the mechanism(s) for nucleation of phases, pinning of order parameter structures and mechanisms for meta-stability of inhomogeneous states of  ${}^3\text{He}$  in aerogel.

Finally, the impregnation of liquid  ${}^3\text{He}$  within an elastic solid with negligible intrinsic dissipation provides a new arena for the study of the collective mode dynamics of superfluid phases. In addition to longitudinal acoustic waves, the solid aerogel provides a mechanism to excite the confined liquid with a bulk transverse current probe. This opens up the possibility of studying new mechanisms for acoustic birefringence that reflect the underlying broken symmetries of the superfluid phases. Will the ground state of superfluid  ${}^3\text{He}$  in aerogel exhibit spontaneous birefringence associated with broken time-inversion symmetry, or broken chiral symmetry? Will short-range anisotropic correlations of the aerogel lead to linear birefringence? Can we tailor new aerogels with chiral properties and induce new types of broken symmetry in the liquid? These are some of the many interesting and challenging directions to pursue in future work.

- 
- [1] D. D. Osheroff, R. C. Richardson, and D. M. Lee, Phys. Rev. Lett. **28**, 885 (1972).
- [2] A. J. Leggett, Phys. Rev. Lett. **29**, 1227 (1972).
- [3] G. Baym and C. J. Pethick, *Landau Fermi-Liquid Theory* (Wiley, New York, 1991).
- [4] V. P. Mineev and K. V. Samokhin, *Introduction to Unconventional Superconductivity* (Gordon and Breach Science Publishers, Amsterdam, The Netherlands, 1999).
- [5] D. VanHarlingen, Rev. Mod. Phys. **67**, 515 (1995).
- [6] T. Löfwander, V. S. Shumeiko, and G. Wendin, Supercond. Sci. Technol. **14**, R53 (2001).
- [7] M. Chan, N. Mulders, and J. Reppy, Physics Today **8**, 30 (1996).
- [8] K. Matsumoto, J. V. Porto, L. Pollack, E. N. Smith, T. L. Ho, and J. M. Parpia, Phys. Rev. Lett. **79**, 253 (1997).
- [9] G. Gervais, K. Yawata, N. Mulders, and W. P. Halperin, Phys. Rev. Lett. **88**, 045505 (2002).
- [10] E. V. Thuneberg, S.-K. Yip, M. Fogelström, and J. A. Sauls, Phys. Rev. Lett. **80**, 2861 (1998).
- [11] J. A. Sauls and P. Sharma, Phys. Rev. B **68**, 224502 (2003).
- [12] J. Porto and J. Parpia, Phys. Rev. Lett. **74**, 4667 (1995).
- [13] D. Sprague, T. Haard, J. Kycia, M. Rand, Y. Lee, P. Hamot, and W. Halperin, Phys. Rev. Lett. **75**, 661 (1995).
- [14] J. Fricke, Sci. Am. **258**, 92 (1988).
- [15] J. Porto and J. Parpia, Phys. Rev. B **59**, 14583 (1999).
- [16] T. M. Haard, G. Gervais, R. Nomura, and W. P. Halperin, Physica B **284-288**, 289 (2000).
- [17] D. Rainer and J. A. Sauls, J. Low Temp. Phys. **110**, 525 (1998).
- [18] A. A. Abrikosov and I. Khalatnikov, Sov. Phys. Uspeki **66**, 68 (1958).
- [19] E. Collin, Ph.D. thesis, Université Joseph Fourier, Grenoble (2002).
- [20] P. Sharma and J. A. Sauls, Physica B **284-288**, 297 (2000).
- [21] A. C. Anderson, W. Reese, and J. C. Wheatley, Phys. Rev. **127**, 671 (1962).
- [22] A. A. Abrikosov and L. P. Gorkov, Sov. Phys. JETP **12**, 1243 (1961).
- [23] G. Lawes, S. Kingsley, N. Mulders, and J. M. Parpia, Phys. Rev. Lett. **84**, 4148 (2000).
- [24] R. Hänninen and E. V. Thuneberg, Phys. Rev. B **67**, 214507 (2003).
- [25] H. Choi, G. Gervais, N. Mulders, and W. P. Halperin, Phys. Rev. Lett. (**submitted**), 4 (2004).
- [26] D. S. Greywall, Phys. Rev. **B33**, 7520 (1986).
- [27] J. C. Wheatley, Rev. Mod. Phys. **47**, 415 (1975).
- [28] S. N. Fisher, A. M. Guénault, A. J. Hale, and G. R. Pickett, J. Low Temp. Phys. **126**, 673 (2001).
- [29] P. Sharma and J. A. Sauls, J. Low Temp. Phys. **125**, 115 (2001).
- [30] S. N. Fisher, A. M. Guénault, A. J. Hale, and G. R. Pickett, Phys. Rev. Lett. **91**, 105303 (2003).
- [31] G. Gervais, T. M. Haard, R. Nomura, N. Mulders, and W. P. Halperin, Phys. Rev. Lett. **87**, 035701 (2001).
- [32] B. I. Barker, Y. Lee, L. Polukhina, D. D. Osheroff, L. W. Hrubesh, and J. F. Poco, Phys. Rev. Lett. **85**, 2148 (2000).
- [33] G. Baramidze and G. Kharadze, J. Phys. Cond. Matt. **14**, 7471 (2002).
- [34] G. Gervais, K. Yawata, N. Mulders, and W. P. Halperin, Phys. Rev. B **66**, 054528 (2002).
- [35] E. Nazaretski, N. Mulders, and J. Parpia, J. Low Temp. Phys. **134**, 763 (2004).
- [36] V. P. Mineev and P. L. Krotkov, Phys. Rev. B **65**, 024501:10pp (2002).
- [37] I. Fomin, Sov. Phys. JETP Lett. **77**, 240 (2003).
- [38] G. Baramidze and G. Kharadze, Physica **284-288**, 305 (2000).